IET Renewable Power Generation

Research Article

IET Journals
The Institution of Engineering and Technology

Optimal expansion planning of isolated microgrid with renewable energy resources and controllable loads

ISSN 1752-1416
Received on 14th July 2016
Revised 2nd March 2017
Accepted on 4th March 2017
E-First on 19th May 2017
doi: 10.1049/iet-rpg.2016.0661
www.ietdl.org

Zhaojian Wang[1], Ying Chen[1] ✉, Shengwei Mei[1], Shaowei Huang[1], Yin Xu[2]

[1]*Department of Electrical Engineering, Tsinghua University, Beijing 100084, People's Republic of China*
[2]*School of Electrical Engineering, Beijing Jiaotong University, Beijing 100044, People's Republic of China*
✉ *E-mail: chen_ying@tsinghua.edu.cn*

Abstract: As the load demand in a microgrid increases, more distributed generators (DGs) should be installed to meet the demand, which makes the microgrid expansion planning very important. To obtain the optimal expansion strategy, a tri-level expansion planning framework is presented for an isolated microgrid in this study, which is composed of demand expansion, capacity optimisation and operation optimisation. The uncertainties of load forecasting are considered. Latin hypercube sampling method is utilised to generate the load demand scenarios. Controllable load is also considered in the expansion, which can be switched off and on as required. Considering the complexity of the operation optimisation problem, particle swarm optimisation is used to obtain the planning results. Finally, numerical simulations for an isolated microgrid in Weizhou Island, Guangxi, China are utilised to validate the effectiveness of the proposed model as well as its solving algorithm.

Nomenclature

Parameter

W	set of wind turbines
S	set of photovoltaics
B	set of batteries
C	set of controllable loads
T_{C}	controllable load permissible shifting time interval
U_i	unit cost of equipment i, $i \in \{W, S, B, C\}$
L_i	life cycle of equipment i, $i \in \{W, S, B, C\}$
r	discount rate
C_{i_inv}	yearly installation costs of equipment i, $i \in \{W, S, B, C\}$
M_i	unit maintenance cost of equipment i, $i \in \{W, S, B, C\}$
C_{i_om}	yearly maintenance costs of equipment i, $i \in \{W, S, B, C\}$
D_i	unit salvage value of equipment i, $i \in \{W, S, C\}$
I_{i_D}	yearly salvage value of equipment i, $i \in \{W, S, C\}$
p_{c_com}	unit trading cost for control rights of controllable loads
C_{C_com}	yearly operation costs for trading control right of controllable loads
$P^n_{C\_loss}$	controllable load loss in the nth planning year
α_{C_pun}	unit compensation for the unplanned controllable load interruption
α_{U_pun}	unit compensation for the unplanned uncontrollable load interruption
C_{C_loss}	yearly operation costs by compensating for controllable load interruption
P^n_{load}	load demand in the nth year
I^n_{op}	yearly operation revenue of the microgrid
$I^n_{\mathrm{op}k}$	yearly operation revenue of the microgrid in scenario k
I^n_{cap}	yearly profit of the microgrid
$I^n_{\mathrm{cap}k}$	yearly profit of the microgrid in scenario k
R_n	reliability of microgrid in the nth year
$R_{\min}$	minimal acceptable reliability
P^n_i	capacities of equipment i, $i \in \{W, S, B, C\}$ in the nth year
$P^n_{i\_D}$	scrapped capacities of equipment i, $i \in \{W, S, B, C\}$ in the nth year
$P^{\max}_i$	maximal capacities of equipment i, $i \in \{W, S, B, C\}$
I^n_{SEL}	yearly income of the energy supplies
$C^n_{U\_loss}$	compensate for uncontrollable load interruption
$C^n_{C\_loss}$	compensate for controllable load interruption
M	large positive value
$\eta_{\mathrm{d}}, \eta_{\mathrm{c}}$	discharging and charging efficiencies of the battery
η_{con}	maximal percentage of controllable load in total load demand
α_p	electricity price
α_s	government subsidy for renewable generation
$S_{\min}$	minimal state-of-charge (SOC) of battery
$S_{\max}$	maximal SOC of battery

Decision variable

ΔP^t_{c-}	controllable load switched off during period t
ΔP^t_{c+}	controllable load switched on during period t
P^n_i	capacities of equipment i, $i \in \{W, S, B, C\}$ in the nth year
P^t_{W}	actual power generated by wind turbines during period t
P^t_{S}	actual power generated by photovoltaics during period t
P^t_{U}	demands from uncontrollable loads during period t
P^t_{C}	demands from controllable loads during period t
ΔP^t_{B+}	power discharged by batteries in the period t
ΔP^t_{B-}	power charged by batteries in the period t
P^t_{cur}	power curtailed in the period t
$P^t_{U\_loss}$	uncontrollable load interruptions in the period t
$\tilde{b}_t, \tilde{c}_t$	binary variables
P^n_{c}	capacities of controllable load in the nth year

1 Introduction

1.1 Motivation

Isolated microgrids are usually used in islands and remote areas to provide power supply [1–3]. As the load demand increases, the microgrid is supposed to be expanded to meet the increasing load demand. A reasonable capacity configuration expansion planning of distributed generators (DGs) and batteries can increase the

economic benefits and enhance the reliability of isolated microgrids at the same time [4–6]. This paper is focused on a real isolated microgrid in Weizhou Island, Guangxi Province, China. In the microgrid, the load demand increases, and the currently available power sources are not able to meet the increased demand. The power shortage restricts the development of the tourism of the district and everyday life of residents. Thus, it is necessary to work out an optimal expansion planning of the microgrid to meet the load demand, and facilitate the economy growth of the island.

1.2 Problem description

The expansion of an isolated microgrid can be achieved by installing more DGs, strengthening and extending local distribution grids, and connecting incremental loads. In the case of Weizhou Island, due to the environment protection restrictions, only renewable DGs can be installed. In addition, because of the intermittent nature of the power supply, it cannot meet the changing load demand. Thus, in order to maintain the power balance within the microgrid, energy storage systems are deployed.

Different from the optimal sizing of microgrid, incremental capacity of devices should be optimised for each planning cycle, e.g. a year. A corresponding investment plan should be made to maximise the profit as well as enhance the reliability of the isolated microgrid over its life cycle. Meanwhile, restricted by the natural environment, the total capacity of renewable DGs that can be installed in the microgrid is limited. As investments on per unit of energy supply increases, the yearly profit of the microgrid will decrease. If the capacity of newly installed DGs is insufficient, the reliability of power supplies will be reduced. When unacceptable service interruptions or negative yearly profit are counted, the expansion of microgrid becomes unreasonable. In addition, optimised operations of energy generation and storage devices can improve the runtime performance of the isolated microgrid, as well as its expansion capability. Thus, the optimisation of short-term microgrid operations should be nested into the long-term expansion planning.

Moreover, integrated with embedded computation and communication apparatuses, loads in microgrid can be controlled according to regulation requirements [7]. When controllable loads are utilised, operational performance of microgrid can be enhanced by reduced appliance investments. Therefore, to prolong the expansion of microgrid, costs and control strategy of controllable loads should be carefully modelled into the optimal planning problem.

1.3 Literature review

In [5], the feasibility between isolated microgrids and grid-connected microgrids is compared using HOMER software. The result implies that grid connection for microgrid is not necessary for energy support but trading of excess electricity. A two-stage planning model is introduced in [8] to determine the optimal planning of combined cooling heating and power (CCHP) microgrid. The first stage is investigating the optimal capacity configuration for equipment. The second stage determines the dispatch strategy using mixed-integer linear programming (MILP), where the microgrid operation is nested into planning. The same idea is also used in [9, 10]. The two-stage model combines capacity configuration optimisation and microgrid operation optimisation together, which describes microgrid planning clearly. However, it is not appropriate for microgrid expansion planning due to not considering load increase year by year.

Planning models considering the uncertainties induced by intermittent DGs are proposed in many studies [4, 9, 11–14]. In [11], many approaches to addressing uncertainties are summarised, such as robust optimisation, probabilistic approach, possibilistic approach and so on. For optimal planning of a microgrid, robust optimisation and probabilistic approaches have been applied to handle uncertainty features of DGs and loads. Robust optimisation is applied in [9, 12, 15]. In [9], forecasting errors in load and renewable generation, and uncertainty in microgrid islanding are considered. In [12], robust optimisation is adopted to determine optimal locations and capacities of DGs, where the uncertainties of DG outputs and load demand are taken into account. In [15], a robust planning methodology is proposed for the integration of DGs, where Monte Carlo is adopted in the solution algorithm by generating random scenarios with variations of weather and load demands. As for the probabilistic approach, sampling methods are widely used to generate different scenarios of uncertain parameters. In [13], Monte Carlo is used to generate scenarios of wind speed, and a scenario reduction method is adopted to decrease the scenarios generated. Mote Carlo simulation is often regarded as an accurate sampling method, however, it tends to be computation-intensive tasks. Latin hypercube sampling (LHS) is an efficient sampling method, which can reduce the simulation runs required effectively [16–18]. Thus, it may reduce the computational expenses for the microgrid expansion.

In power system, many loads are flexible [19, 20], such as washing machines, refrigerators, water heaters and electrical vehicles. General models of three different types of time-shiftable load models are proposed in [21]. These load demands are time-shiftable, which makes it possible for consumers to participate in power system operation [22]. Microgrid scheduling is studied in [23], where the microgrid is assumed to be equipped with smart appliances to make the load shiftable. In [10], a simple controllable load model is considered in microgrid optimal design, where controllable load is switched off and on as needed. Heating/cooling systems are included in microgrid planning in [24], which are controllable to some extent. They can improve the economy efficiency and reliability of microgrid. Thus, it is of great importance to propose a general model of controllable load in microgrid planning.

1.4 Contributions

Optimal expansion planning has two purposes, i.e. seeking the maximum acceptable load demand and finding the optimal installation plan for renewable DGs, batteries, and controllable loads. In this paper, a tri-level expansion planning framework for isolated microgrids is proposed. The salient features of this paper are as follows:

- Controllable loads are modelled for microgrid planning, including both operational and economic models. In addition, results of different permissible shifting time intervals of controllable load are investigated in case studies.
- A tri-level planning framework is proposed to obtain the optimal expansion strategy, which includes demand expansion, capacity optimisation, and operation optimisation.
- Uncertainties of load forecasting are considered, and LHS is utilised to generate load demand scenarios. The impact of load forecasting uncertainties on the annual profit is also investigated in case studies.
- A particle swarm optimisation (PSO)-based algorithm is proposed to obtain the optimal expansion planning strategy, which contains three sub-routines corresponding to the tri-level planning framework.

1.5 Paper organisation

The remaining of this paper is organised as follows. In Section 2, controllable load models are introduced. In Section 3, the tri-level planning model is described in detail. A solution algorithm is then introduced in Section 4, including the decomposition method and PSO. Case studies of a real microgrid are illustrated in Section 5. The conclusions are given in Section 6.

2 Model of controllable load

In the power system, to make load controllable, direct load control (DLC) and pricing-based approaches can be applied [7]. The first one is usually contract-based, i.e. by signing up for the contract, customers give operators the option to remotely switch on or off appliances if needed, and receive compensations for this participation [7]. In the second approach, the operator controls loads indirectly by sending price signals [25]. Due to time-varying

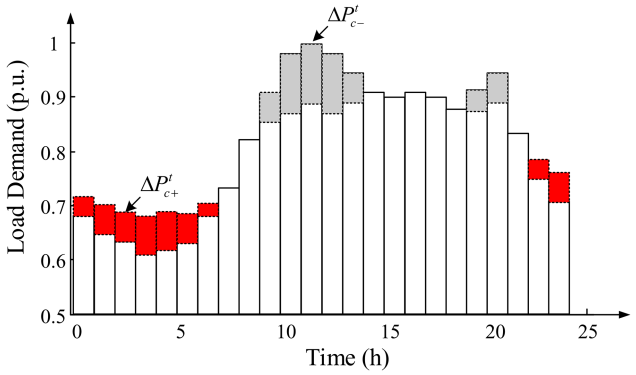

Fig. 1 *Load demand curve after considering controllable loads*

prices, customers may be induced to make smart decisions, e.g. shifting some power usage from high-price periods to low-price periods. As the only number of loads is monitored and controlled, the DLC tends to be an efficient and effective method in a microgrid. In this section, a general model of DLC controllable loads is introduced, which describes their time-shiftable feature, as well as installation and operation costs.

2.1 Operation of controllable load

Smart appliances are being embedded into existing or emerging loads. These technologies enable remote and direct controls of general loads. By investing on smart appliances, microgrid operators can adopt the DLC during daily operations. By DLC, the controllable load can be switched off in peak hours and switched on in off-peak hours during a period T_C, which is called as load shifting. T_C is called as controllable load permissible shifting time interval. If T_C is large, it means that the controllable loads are permitted to shift in a long time intervals.

Fig. 1 illustrates a daily demand curve of microgrid with load shifting, where the $T_C = 24$ h. In Fig. 1, grey bars refer to the load that is switched off during peak hours while red bars represent the load that is switched on in the off-peak hours. Denote the amount of controllable load that is switched off and on during period t by ΔP^t_{c-} and ΔP^t_{c+}, respectively. If there is no controllable load switched on or off, then $\Delta P^t_{c-} = \Delta P^t_{c+}$. Since the load demand is just moved from one period to another, the total load demand within the period remains unchanged. However, due to uncertain outputs of intermittent DGs, load shifting may cause supply interruptions, which means

$$\sum_{t=1}^{24} \Delta P^t_{c-} \geq \sum_{t=1}^{24} \Delta P^t_{c+} \tag{1}$$

Then, compensations to customers should be issued for the violation of reliability commitments, which increase the operation cost of the microgrid and reduce the benefit of DLC at the same time. Actually, for interruptible type loads, (1) still is applicable by setting $\Delta P^t_{c+} = 0$.

2.2 Costs of controllable loads

To make load controllable, smart appliances should be installed, which results in investment cost, maintenance cost, and salvage value. Moreover, customers may be not willing to let microgrid operator switch on or off the load, so some compensations are needed to obtain the control right. In addition, compensation will occur if controllable loads are not supplied. In this subsection, we will introduce these costs in detail.

- Yearly installation costs of smart appliances embedded in conventional loads

$$C_{C\_inv} = U_C P_C \frac{r(1+r)^{L_C}}{(1+r)^{L_C} - 1} \tag{2}$$

where for each controllable load, U_C is the unit cost (CNY/kW) of smart appliances, P_C is the controllable load capacity, L_C denotes the life cycle, and r stands for the discount rate. Equation (2) is the equivalent annual cost of the appliances [26].

- Yearly maintenance costs of controllable loads

$$C_{C\_om} = M_C P_C \tag{3}$$

where M_C is the unit maintenance cost (CNY/kW) of controllable loads.

- Yearly salvage value of controllable loads

$$I_{C\_D} = P_C D_C \frac{r}{(1+r)^{L_C} - 1} \tag{4}$$

where D_C is the unit salvage value (CNY/kW).

- Yearly operation costs for trading control right of controllable loads from customers

$$C_{C\_com} = p_{c\_com} P_C \tag{5}$$

where p_{c_com} represents the unit trading cost (CNY/kW) for control rights of controllable loads. It should be noted that there are different ways for pricing the control right of shiftable loads. The operator of the microgrid should establish contracts with customers using these loads, which have been widely adopted in demand response applications. Especially, in (5), costs for trading control right are determined by the capacity of controllable loads. Other trading methods can also be used, e.g. it could be charged according to daily control frequencies.

- Yearly operation costs caused by compensation for controllable load supply interruptions.

Load supply interruptions are accounted as follows:

$$P^n_{C\_loss} = \sum_{\tau=0}^{(8760/T_C)-1} \sum_{k=1}^{T_C} \Delta P^{\tau \times T_C + k}_{C-} - \Delta P^{\tau \times T_C + k}_{C+} \tag{6}$$

where $P^n_{C\_loss}$ is the controllable load loss in the nth planning year. Then, the corresponding compensations are given as

$$C_{C\_loss} = \alpha_{C\_pun} P^n_{C\_loss} \tag{7}$$

where α_{C_pun} stands for unit compensation (CNY/kWh) for the unplanned power supply interruption.

In fact, (7) is only one acceptable type of compensation mechanism, and other types may also exist in reality. For example, in some situation, compensation will be given periodically once the load joins the daily control of the host microgrid.

3 Expansion planning for isolated microgrids

3.1 Overview of expansion planning

The following work is based on some reasonable assumptions about expansions of the isolated microgrid system, including: (i) load demand increases yearly with a predictable rate; (ii) power generations of renewable energy resources are varying along with weather conditions, which can be described by scenario based simulations; (iii) installation and maintenance cost and salvage income of equipment are proportional to their capacity; and (iv) the equivalent annual cost model is used to even yearly investments on variant devices in this work, which keeps the yearly profit of the microgrid stable in its lifespan.

To obtain optimal expansion results, a tri-level expansion planning framework for isolated microgrids is proposed. The

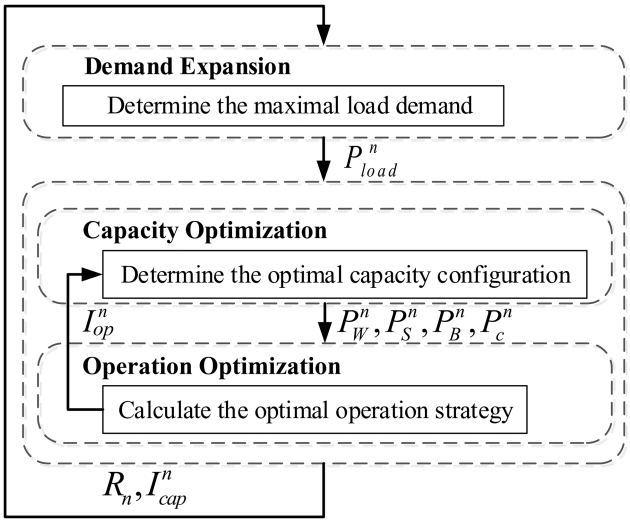

Fig. 2 *Tri-level planning framework*

framework is composed of three layers, which are demand expansion, capacity optimisation and operation optimisation. The demand expansion layer is to obtain the maximum load demand that the microgrid can supply, where the load forecast is given in advance. Capacity optimisation layer will determine the capacities of devices in each planning year. Nested in the capacity optimisation, operation optimisation layer is used to emulate the optimal operation of the microgrid in each planning year. The relationship and interfaces between the above three layers are shown in Fig. 2.

In Fig. 2, P^n_{load} is the load demand in the nth year. $P^n_{\text{W}}, P^n_{\text{S}}, P^n_{\text{B}}, P^n_{\text{c}}$ stand for the total capacities of wind turbines (WTs), photovoltaic (PV) panels, storages and controllable load in the nth year. $I^n_{\text{op}}, I^n_{\text{cap}}$ are yearly operation revenue and yearly profit of the microgrid, respectively. R_n is the reliability index in the nth year.

In the demand expansion layer, R_n and I^n_{cap} are adopted as criteria to determine whether the expansion should be stopped. P^n_{load} is given to capacity optimisation layer as the new load demand. Then capacities of new devices, including renewable energy resources, storages and controllable loads will be obtained by solving the capacity optimisation problem. Nested in the capacity optimisation, optimal operations of the microgrid are simulated. Generally, operations of devices in microgrid are optimised to enhance its efficiency and reliability over successive scenarios, which describes hourly variations of weather conditions and load demands according to their statistical characteristics. After optimal capacities of controllable loads and other devices are obtained, they would become the initial condition for the optimal expansion planning of the next year.

The proposed tri-level planning framework represents three different perspectives towards the microgrid expansion. The demand expansion stands for the investor, who is concerned the expansion result. The capacity optimisation represents the microgrid planner, who determines the optimal upgrade of devices during the planning process. The operation optimisation stands for the microgrid operator, who designs the best operation strategy.

3.2 Demand expansion layer

In this layer, the expansion results are obtained, including: (i) the maximum load demand that the microgrid can supply; (ii) when the expansion stops. To determine whether the expansion process should be terminated, two criteria are adopted. The first criterion is that the reliability index should be higher than a preset level, i.e. $R_n \geq R_{\min}$, where $R_{\min}$ is the minimal acceptable reliability. The second criterion is that the expected yearly profit should be positive, i.e.$I^n_{\text{cap}} \geq 0$. If any of the two criteria is violated, the expansion should be terminated.

The reliability index of microgrid in the nth year is defined as follows:

$$R_n = \left(\sum_{t=1}^{T} P^t - \sum_{t=1}^{T} P^t_{\text{loss}}\right) / \sum_{t=1}^{T} P^t \tag{8}$$

where P^t_{loss} is the total load interruption during hour t including controllable load loss and uncontrollable load loss, and P^t is the load demand during hour t, $T = 8760$ denotes the 8760 h in one year. The reliability definition in (8) is derived from the concept of expected energy not supplied [27], whose definition can be referred to [4]. The uncontrollable load loss is calculated every hour, while controllable load loss is calculated at the end of every time interval T_{C}, as given in (6). In the reliability index calculation, we only need to balance the controllable load in one day instead of every hour, which is one of the advantages of controllable load.

In addition, since the load forecasting is not very accurate, uncertainties should include. In general, the long-term load forecasting obeys normal distribution [28]. Then, we can generate scenarios of error of load demand by sampling. LHS is an efficient sampling method that ensures each probability distribution is evenly sampled [16, 17], which is adopted for generating scenarios with varied yearly incremental load demands for optimal expansion planning. In the nth planning year, all of the scenarios are given to the capacity optimisation layer. Then, different profits will be obtained in each scenario denoted as $I^n_{\text{cap}k}$, the expectation of which is denoted as the final profit I^n_{cap}.

3.3 Capacity optimisation layer

For an isolated microgrid, its economic efficiency is measured by its yearly profit, which is determined by its yearly income and cost. The income mainly comes from power supplies to loads, including operation profit and yearly salvage value. Its costs are mainly composed of investment cost and maintenance cost. In each load demand scenario, the model of capacity optimisation is as follows:

$$\max I^n_{\text{cap}k} = I^n_{\text{op}k} - \sum_i \left(C_{i\_inv} + C_{i\_om} - I_{i\_D}\right) \tag{9a}$$

$$\text{s.t.} \quad P^{n-1}_{\text{W}} - P^n_{W\_D} \leq P^n_{\text{W}} \leq P^{\max}_{\text{W}} \tag{9b}$$

$$P^{n-1}_{\text{S}} - P^n_{S\_D} \leq P^n_{\text{S}} \leq P^{\max}_{\text{S}} \tag{9c}$$

$$P^{n-1}_{\text{B}} - P^n_{B\_D} \leq P^n_{\text{B}} \leq P^{\max}_{\text{B}} \tag{9d}$$

$$P^{n-1}_{\text{c}} \leq P^n_{\text{c}} \leq P^{\max}_{\text{c}} \tag{9e}$$

$$P^n_{\text{W}}, P^n_{\text{S}}, P^n_{\text{B}}, P^n_{\text{c}} \geq 0 \tag{9f}$$

where $i \in \{W, S, B, C\}$ resembles WT, PV, battery and controllable load. Optimisation variables are $P^n_{\text{W}}, P^n_{\text{S}}, P^n_{\text{B}}, P^n_{\text{c}}$. Here, the upper index n is for the nth planning year. $P^n_{W\_D}, P^n_{S\_D}, P^n_{B\_D}$ are scrapped capacities of WT, PV and battery in the nth year. $P^{\max}_{\text{W}}, P^{\max}_{\text{S}}, P^{\max}_{\text{B}}, P^{\max}_{\text{c}}$ are the maximal capacities of WT, PV, battery and controllable load.

3.3.1 Objective function: In (9a), $C_{i\_inv}, C_{i\_om}, I_{i\_D}$ are the corresponding yearly installation cost, yearly maintenance cost and yearly salvage value of WT, PV, battery and controllable load. The calculations of $C_{i\_inv}, C_{i\_om}, I_{i\_D}, i \in \{W, S, B\}$ are similar to (2)–(4), which are omitted due to space limit. In addition, salvage value of battery is assumed to be zero, i.e. $I_{B\_D} = 0$. Suppose the number of scenarios is K, then $I^n_{\text{cap}} = (1/K)\sum_{k=1}^{k=K} I^n_{\text{cap}k}$.

3.3.2 Constraints: Constraints (9b)–(9d) are capacities limit constraints of DGs. In these constraints, we consider the scrap of

equipment, which is denoted by $P^n_{i\_D}, i \in \{W, S, B\}$. $P^n_{i\_D}$ is equal to the capacities invested $n - L_i$ years ago, where L_i denotes the life cycle of corresponding appliances. Constraint (9e) is the power constraint of controllable load. As the life cycle of smart appliance is usually very long, its scrap is not considered.

Established models of WT, PV and battery are adopted. WT and battery models are referred to [26], and PV model can be found in [29].

3.4 Operation optimisation layer

In this work, optimal controls to devices in microgrid are updated for each hour. Moreover, for the sake of simplification, the weather conditions and demands from loads are regarded as constant in each hour, as well as the power input and output from renewable energy resources and batteries. Then, the hourly energy balance in the microgrid is simplified as power balance among energy sources, loads and storages.

The yearly operation optimisation of the isolated microgrid system can be represented as

$$\max I^n_{\text{op}k} = I^n_{\text{SEL}} - C^n_{U\_loss} - C^n_{C\_loss} \tag{10a}$$

$$\text{s.t.} \quad P^t_{\text{W}} + P^t_{\text{S}} + \Delta P^t_{B+} - \Delta P^t_{B-} - P^t_{\text{curtail}} = P^t_{\text{U}} + P^t_{\text{C}} + \Delta P^t_{C+} - \Delta P^t_{C-} - P^t_{U\_loss}, \quad \forall t \tag{10b}$$

$$0 \le P^t_{\text{curtail}} \le P^t_{\text{W}} + P^t_{\text{S}} \tag{10c}$$

$$0 \le P^t_{U\_loss} \le P^t_{\text{U}} \tag{10d}$$

$$0 \le \Delta P^t_{C-} \le P^t_{\text{C}}, \quad \forall t \tag{10e}$$

$$P^t_{\text{C}}/(P^t_{\text{C}} + P^t_{\text{U}}) \le \eta_{\text{con}} \tag{10f}$$

$$0 \le \Delta P^t_{C+} \le M\tilde{c}_t, \quad \forall t \tag{10g}$$

$$0 \le \Delta P^t_{C-} \le M(1 - \tilde{c}_t), \quad \forall t \tag{10h}$$

$$0 \le \Delta P^t_{B+} \le M\tilde{b}_t, \quad \forall t \tag{10i}$$

$$0 \le \Delta P^t_{B-} \le M\left(1 - \tilde{b}_t\right), \quad \forall t \tag{10j}$$

$$\sum_{\tau=1}^{T_{\text{C}}} \Delta P^{kT_{\text{C}}+\tau}_{c-} \ge \sum_{\tau=1}^{T_{\text{C}}} \Delta P^{kT_{\text{C}}+\tau}_{c+}, \quad k = 0, 1, \ldots, \frac{8760}{T_{\text{C}}} - 1. \tag{10k}$$

$$S_{\min} P^n_{\text{B}} \le S_{\min} P^n_{\text{B}} - \sum_{\tau=1}^{t-1} \eta_d \Delta P^{\tau}_{B+} + \sum_{\tau=1}^{t-1} \eta_c \Delta P^{\tau}_{B-} \le S_{\max} P^n_{\text{B}}, \quad t > 1 \tag{10l}$$

$$R_n \ge R_{\min} \tag{10m}$$

where $t = 1, 2, \ldots, 8760$ denotes each hour in one year, $S_{\min}$ and $S_{\max}$ are minimal and maximal SOC of the battery, respectively. I^n_{SEL} represents the yearly income of the energy supplies. $C^n_{U\_loss}, C^n_{C\_loss}$ are compensate for uncontrollable load and controllable load, respectively. Optimisation variables include $\Delta P^t_{B+}, \Delta P^t_{B-}, P^t_{\text{curtail}}, \Delta P^t_{C-}, \Delta P^t_{C+}$ and $P^t_{U\_loss}$, which stand for power discharged and charged by batteries, power curtailed, controllable load switched off and switched on and uncontrollable load interruptions in the period t, respectively. $P^t_{\text{W}}, P^t_{\text{S}}, P^t_{\text{U}}, P^t_{\text{C}}$ denote actual power generated by WT and PV, and demands from uncontrollable and controllable loads during period t in the nth planning year respectively. $\eta_{\text{d}}, \eta_{\text{c}}$ are discharging and charging efficiency of the battery. η_{con} is the maximal percentage of controllable load in total load demand. $\tilde{b}_t \in \{0, 1\}, \tilde{c}_t \in \{0, 1\}$, and M is a large positive value. The details about (10a)–(10l) are listed as follows.

3.4.1 Objective function:

- Yearly income of power selling. The power selling P^t_{SEL} during period t is calculated as

$$P^t_{\text{SEL}} = P^t_{\text{U}} + P^t_{\text{C}} + \Delta P^t_{C+} - \Delta P^t_{C-} - P^t_{U\_loss} \tag{11}$$

  Yearly power selling income consists of electricity selling and government subsidy for renewable energy

$$I_{SEL} = \sum_{t=1}^{T} (\alpha_p + \alpha_s) P^t_{\text{SEL}} \tag{12}$$

  where α_p (CNY/kWh) is the electricity price, α_s (CNY/kWh) is the government subsidy for renewable generation, $T = 8760$.
- Yearly uncontrollable load interruption compensation. Compensation for load interruption is modelled as follows:

$$C_{U\_loss} = \sum_{t=1}^{T} \alpha_{U\_pun} P^t_{U\_loss} \tag{13}$$

  where α_{U_pun} (CNY/kWh) is the unit compensation cost for load interruptions.

3.4.2 Constraints: Constraint (10b) represents the energy balance in microgrid during period t. Capacity of curtailed power is limited as shown in (10c). Constraint (10d) gives the capacity limit of uncontrollable load interruptions. Constraint (10e) limits the capacity of controllable loads that can be switched off. Constraint (10f) limits the percentage of controllable loads in the overall load. Constraints (10g) and (10h) indicate that ΔP^t_{c-} and ΔP^t_{c+} cannot be positive at the same time. Constraints (10i) and (10j) indicate that ΔP^t_{B-} and ΔP^t_{B+} cannot be positive at the same time. Constraint (10k) is derived from (1). The constraint (10l) describes the limits of the battery SOC, which is determined by the charging status in all the former periods.

It can be seen that the operation optimisation concerned is modelled as an MILP problem. By introducing binary variables for batteries, efficiencies of charging and discharging are considered carefully. Modelled by two variables, controllable loads switched on and off are accounted separately, which may have different cost functions theoretically. Moreover, the binary variable $\tilde{c}_t$ is adopted in constraints (10g) and (10h), which ensure correct action sequences of controllable loads.

4 Solution of expansion planning

To obtain the optimal expansion plan of the isolated microgrid, the proposed tri-level optimisation problem is solved by master and sub-problem iterations, as shown in Fig. 3.

It can be seen from Fig. 3 that three sub-routines are created to emulate the optimal decision process for the tri-level expansion optimisation. The functions and inter-operations of sub-routines are explained as follows.

4.1 Demand expansion optimisation sub-routine

With capacity configurations of DGs, batteries and loads in the previous year, e.g. $n - 1$th planning year concerned, the microgrid expansion plan is optimised sequentially for the nth year, which decides the capacities of newly installed devices according to increased local loads. Then, the power supply reliability and efficiency of the isolated microgrid are evaluated, i.e. R_n, I^n_{cap} given

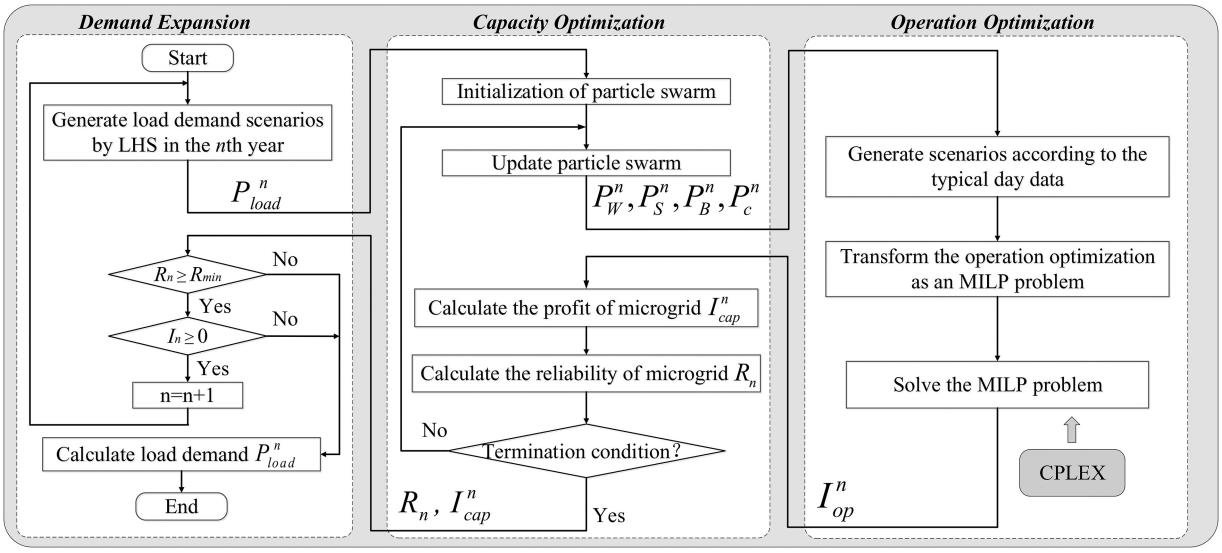

Fig. 3 *Solution of the tri-level expansion planning*

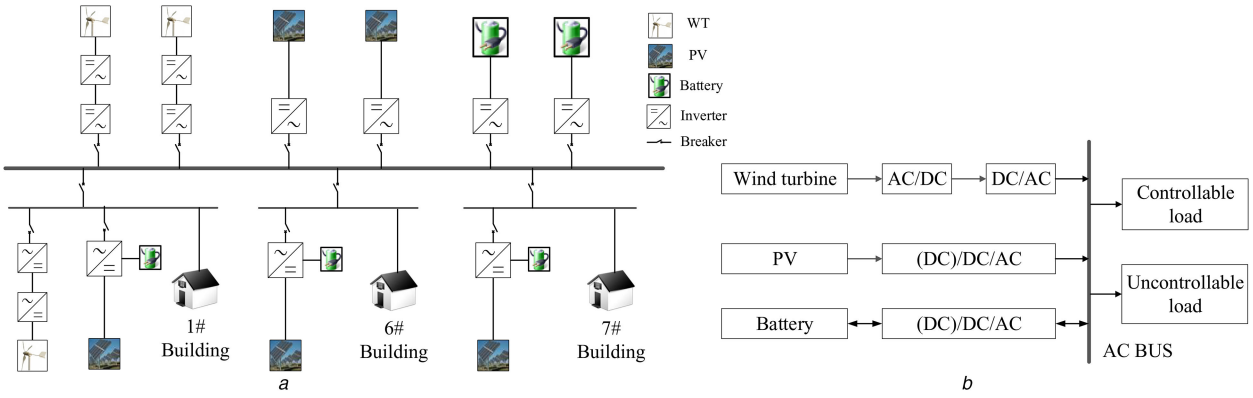

Fig. 4 *Microgrid topology*
(a) Electric connection diagram, ***(b)*** Structure of the microgrid

in (8) and (9a). If yearly performance of the microgrid is acceptable, the demand expansion with the same pattern can be expected for the next year. Otherwise, the microgrid should stop integrating new loads and corresponding investments. The optimal capacities of DGs, batteries and controllable loads in *n*th year are given by executing the capacity optimisation sub-routine.

4.2 Device capacity optimisation sub-routine

In this sub-routine, a PSO-based optimisation method is adopted to determine installed capacities of concerned devices [6]. First, candidate particles for searching optimal solution are defined by varied total capacities of wind generators, PVs, batteries and controllable loads, i.e. $P^n_{\mathrm{W}}, P^n_{\mathrm{S}}, P^n_{\mathrm{B}}, P^n_{\mathrm{c}}$. Then, for each particle, the corresponding optimal operation of the microgrid can be emulated, from which the yearly operational profit I^n_{op} is obtained. By updating the value and speed of particles according to [30], best capacity configurations for yearly profit I^n_{cap} are searched, which is calculated by (9a). When iterations are larger than 20 and the difference of optimal I^n_{cap} between two iterations is smaller than 0.1%, the capacity optimisation is terminated. The outputs of capacity optimisation sub-routine include not only devices capacities and yearly profit I^n_{cap}, but also the reliability index R_n evaluation of the planning year.

In fact, long-term microgrid planning is a very complex problem and is influenced by uncertainties, which makes it difficult to get a global optimal solution. It can only provide the microgrid owner with an estimation of the microgrid investment and profit. In this perspective, the solution method should be easy to implement. PSO is suitable due to it is relative simple and give us an almost optimal solution rapidly.

4.3 Microgrid operation optimisation sub-routine

In operation optimisation sub-routine, scenarios are generated according to the typical day data. Then, the yearly operation optimisation of microgrid is transformed as an MILP problem, which is solved by existing commercial softwares, such as CPLEX. Then, I^n_{op} is obtained and returned to capacity optimisation sub-routine.

5 Case studies

5.1 Test system

The structure of the test microgrid is shown in Fig. 4, which is a real microgrid on Weizhou Island (21°N, 109.2°E). Fig. 4*a* shows the electric connection diagram of the microgrid. There are three buildings, which contains controllable load and uncontrollable load. Since we mainly focus on the capacity of the DGs, batteries and load demands. The topology structure of the microgrid is simplified to a single-bus system as shown in Fig. 4*b*, where WTs, PV panels and batteries are connected to the AC bus through inverters, respectively. Controllable and uncontrollable loads are both connected to AC bus directly.

The unit capacity of a WT generator is 10 kW. The minimal installation of PV is set as 10 kW, while minimal capacity of a battery is 10 kWh. As mentioned before, due to the lack of space, maximal capacities of the WTs and PV panels are limited as $P^{\max}_{\mathrm{W}} = 150\,\mathrm{kW}$ and $P^{\max}_{\mathrm{S}} = 150\,\mathrm{kW}$. The maximal percentage of controllable load is 20%. $R_{\min}$ is set as 99%.

Table 1 Parameters used in the simulation

System parameters	Value	System parameters	Value
U_S (CNY/kW)	7000	U_W (CNY/p.u.)	40,000
L_S (a)	20	L_W (a)	20
M_S (CNY/kW)	70	M_w (CNY/kW)	40
D_S (CNY/kW)	700	D_W (CNY/p.u.)	4000
U_C (CNY/kW)	300	U_B (CNY/kWh)	3000
M_C (CNY/kW)	10	M_B (CNY/kWh)	15
D_C (CNY/kW)	50	p_{c_com} (CNY/kW)	500
L_C (a)	20	L_B (a)	10
α_{C_pun} (CNY/kWh)	20	α_{U_pun} (CNY/kWh)	20
α_s (CNY/kWh)	0.5	r	0.05
S_{min}	0.4	S_{max}	0.9
α_p (CNY/kWh)	0.5		

Typical hourly wind speed and solar power are illustrated in Figs. 5*a* and *b*, respectively. These data are obtained from meteorological station in Weizhou Island. In the following tests, variations of wind speed from one year to another are not considered for simplifications. In fact, if long-term forecasts of yearly wind speeds are available, the proposed expansion planning can utilise them smoothly by changing wind speed configurations at the beginning of each planning year. Load demand is illustrated in Fig. 5*c*. It is assumed that load demand increases every year. The yearly increasing rate of load forecasting is set as 15%. The forecasting error obeys Gaussian distribution with expectation 0 and standard deviation $\sigma = 0.2$. The simulation runs in the LHS is set as 500. In the optimisation problem (10), we formulate the problem in 8760 h. However, as Weizhou Island is in the tropics, climate does not change greatly in one year. Hence, we ignore the seasonality of this island and use one typical day scenario in the simulation. It should be noted that our model is also applicable when seasonality of production and demand are considered.

All the simulations are implemented using MATLAB R2013a and CPLEX 12.6 at Intel Core i5 2.39 GHz with 8 GB memory. Other parameters used in thispaper are listed in Table 1.

In Table 1, U_i, M_i, D_i, $L_i, i \in \{W, S, B, C\}$ are unit investment cost, unit maintenance cost, unit salvage value and life cycles of equipment, respectively. α_{C_pun} and α_{U_pun} are determined by the loss of power unsupplied, which is correlated to the local area gross domestic product (GDP) of per kWh electricity. For different sites, they could be varied intensively. In Weizhou Island, we set $\alpha_{C\_pun} = \alpha_{U\_pun} = 20$.

5.2 Expansion results considering controllable loads

Based on the proposed tri-level planning framework, yearly expansions of the microgrid on Weizhou Island are optimized with considerations of controllable loads, and results are listed in Table 2.

From Table 2, it can be seen that P_W and P_S reach upper limits in the 8th and 12th planning years, respectively. Although there are no further investments on power generations, the microgrid still can serve the newly installed loads by increasing capacities of batteries and controllable loads. Note that yearly reliability index of the microgrid almost keeps the level of R_{min}. This is due to the optimal operation of batteries and controllable loads, which enhance the time-shifting of energy supplies and consumptions. However, as investments of newly installed devices overwhelm gains from the incremental load supplies, yearly profit of the microgrid continues decreasing after 11th planning year, where the

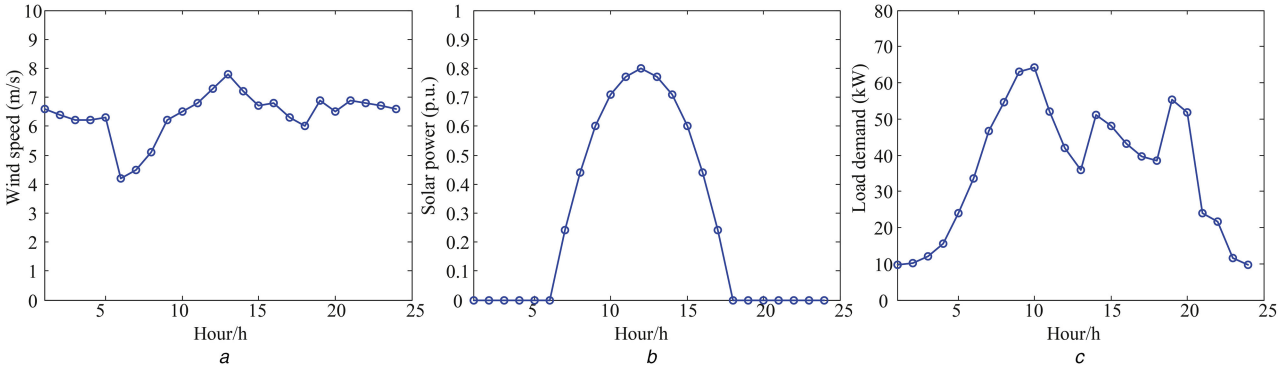

Fig. 5 *Wind speed, solar power and load demand curves*
(a) Wind speed curve, ***(b)*** Solar power curve, ***(c)*** Load demand curve

Table 2 Results with controllable load

n	P_W, kW	P_S, kW	P_B, kWh	P_C, %	R_n, %	I^n_{cap} (10^5 CNY)
1	110	60	120	0	99.29	2.96
2	120	60	160	7.35	99.99	3.31
3	130	70	160	16.5	99.99	3.71
4	130	80	170	20	99.29	4.06
5	140	90	170	20	99.99	4.48
6	140	100	170	20	99.80	4.86
7	150	110	170	20	99.99	5.13
8	150	120	170	20	99.99	5.53
9	150	130	170	20	99.36	5.95
10	150	130	220	20	99.77	6.33
11	150	140	220	20	99.01	6.71
12	150	150	680	20	99.00	5.30
13	150	150	1280	20	99.06	3.31
14	150	150	1900	20	99.00	1.22
15	150	150	2530	20	99.02	−0.89

battery capacity increases dramatically In the 15th year, negative annual profit is observed. Therefore, demand expansion of the microgrid should be stopped at the end of 14th year.

If the full lifespan profit is considered during the optimal expansion of the microgrid, the 11th planning year is obviously the best choice to stop plugging in new loads. After that, the microgrid can remain high-level yearly profit in the rest of its lifespan.

To investigate costs of the controllable load in daily operations, we investigate its switching frequency. The simulation scenario is set in the 9th year. Capacity configuration and controllable load percentage are given in Table 2. Then, Fig. 6 shows the colours out switching actions of the controllable load in one typical day. The blue bars represent the controllable load switched off, and the brown bars represent the controllable load switched on. The x-coordinate represents 24 h in one day, and the y-coordinate is the load demands switched on or switched off.

Compared with Fig. 5, it can be seen that controllable load is switched off when renewable generations are relatively small and load demand is high. For example, many loads are switched off from 5 am to 9 am, when load demand rise gradually while the wind and solar energy are relatively small. On the contrary, the controllable load is switched on when generations are high and load demand is small. For example, at 12 am, many controllable loads are switched on when the wind and solar generations reach their peaks and load demands are small. Thus, it can be concluded as that the switching frequency of the controllable load is influenced by variations of energy adequacy and load demand of the studied microgrid.

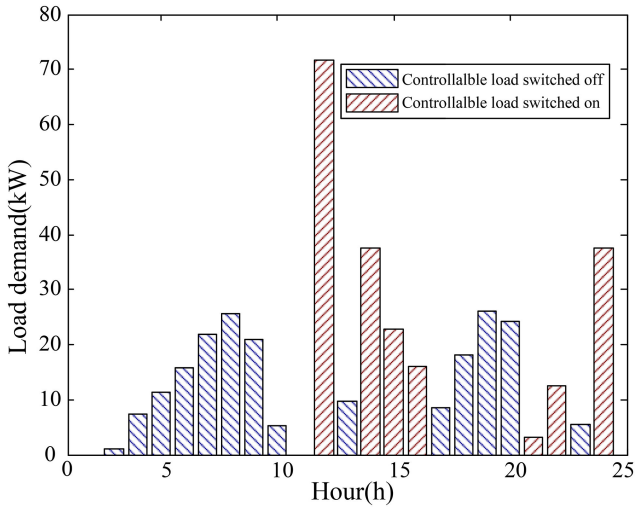

Fig. 6 *Controllable load switched off and switched on*

5.3 Influences of controllable loads on microgrid expansion

Without controllable loads, the microgrid will have a quite different expansion scheme, which is shown in Table 3.

In Table 3, when controllable loads are not considered, all DGs reach upper limits in the 6th planning year, where the load demand increases to 1.9 times. In the 14th planning year, the microgrid encounters a negative yearly profit due to its continuous expansion.

Comparing results in Tables 2 and 3, it can be seen that investments on controllable loads delay installing new DGs for demand expansions. Since energy consumptions cannot be time-shifted, more batteries are required to maintain reliable load supply. Without using controllable loads, the yearly installation capacity of batteries increases far more rapidly than that listed in Table 2. Especially, in the 11th year, 790 kWh batteries are required to keep the microgrid's reliability as 99.05%, while only 220 kWh batteries are needed for the same reliable demand expansion. Moreover, yearly profits of microgrid are also decreased remarkable, and the decrease rates are over 25% in the 11th and 12th years while it exceeds 40% rate in the 13th year. The worst is in the 14th year, where profit decreases 260.66%. Hence, it is shown that controllable loads play important roles in enhancing the profit and loading capability of the microgrid.

5.4 Variation of load forecasting standard deviation

In this subsection, the influence of load forecasting standard deviation σ on profit is investigated, where two scenarios are considered. That is, the σ varies -10 and $+10\%$, respectively. The profits of different scenarios and errors are shown in Table 3.

In Table 4, I_{cap}^{n} with $\sigma = 0.2$ is treated as the base value. According to Table 4, it can be seen that the absolute errors of yearly profits are smaller than 3% in most planning years when P_{W} and P_{S} do not reach upper limits. This indicates that the load forecasting variance has little impact on the microgrid profit if P_{W} and P_{S} do not reach upper limits. On the contrary, absolute errors are prominent and remarkably increased in the last few year when P_{W} and P_{S} reach their upper limits. The reason of above non-linear influences of load forecasting errors is that the yearly profit is more sensitive to the incremental load when capacities of DGs are saturated. This coincides with results in Table 2, where the profit decreases dramatically as load increases in the similar situation.

5.5 Variation of controllable load permissible time interval

In this subsection, the influences of T_{C} on profit and reliability are investigated. Microgrid profit with different T_{C} are shown in Table 5.

As shown in Table 5, as T_{C} increases, the yearly profit will also increase. The profit difference between $T_{\text{C}} = 12$ and $T_{\text{C}} = 24$ is very small. However, the difference between $T_{\text{C}} = 24$ and $T_{\text{C}} = 4$

Table 3 Results without controllable load

n	P_{W}, kW	P_{S}, kW	P_{B}, kWh	R_{n}, %	I_{cap}^{n} (10^5 CNY)	Profit decrease, %
1	80	100	200	99.99	2.53	14.53
2	80	150	200	99.99	2.77	16.31
3	80	150	200	99.99	3.33	10.24
4	120	150	200	99.99	3.75	7.64
5	130	150	200	99.99	4.27	4.69
6	150	150	200	99.96	4.75	2.26
7	150	150	210	99.01	5.13	0
8	150	150	280	99.56	5.46	1.27
9	150	150	330	99.04	5.72	3.87
10	150	150	560	99.19	5.33	15.80
11	150	150	790	99.05	4.88	27.27
12	150	150	1180	99.01	3.79	28.49
13	150	150	1760	99.03	1.91	42.30
14	150	150	2420	99.55	−1.96	260.66

Table 4 Profit with different load forecasting standard deviation

	$\sigma = 0.18$		$\sigma = 0.2$	$\sigma = 0.22$	
n	I^n_{cap} (10^5CNY)	Error, %	I^n_{cap} (10^5CNY)	I^n_{cap} (10^5CNY)	Error, %
1	2.92	−1.35	2.96	2.9	−2.02
2	3.31	0	3.31	3.3	−0.30
3	3.67	−1.07	3.71	3.66	−1.34
4	4.08	0.49	4.06	4	−1.47
5	4.48	0	4.48	4.45	−0.66
6	4.86	0	4.86	4.84	−0.41
7	5.09	−0.77	5.13	4.98	−2.92
8	5.44	−1.62	5.53	5.41	−2.16
9	5.93	−0.33	5.95	5.96	0.16
10	6.16	−2.68	6.33	6.15	−2.84
11	6.53	−2.68	6.71	6.52	−2.83
12	5.08	−4.15	5.3	5.11	−3.58
13	3.53	6.64	3.31	3.12	−5.74
14	1.12	−8.19	1.22	1.33	9.01

Table 5 Profit of different T_C

n	$T_C = 4$	$T_C = 12$	$T_C = 24$
1	2.71	2.72	2.96
2	3.21	3.25	3.31
3	3.53	3.59	3.71
4	3.85	4.03	4.06
5	4.30	4.42	4.48
6	4.78	4.81	4.86
7	5.09	5.13	5.13
8	5.49	5.53	5.53
9	5.81	5.95	5.95
10	5.89	6.33	6.33
11	5.29	6.56	6.71
12	3.88	5.30	5.30
13	1.93	3.31	3.31
14	0.08	1.22	1.22

Table 6 Reliability of different T_C

T_C	2	4	6
reliability (%)	94.86	96.13	97.76
T_C	8	12	24
reliability (%)	97.78	99.77	99.77

is much bigger after the ninth year, where the capacities of WTs and PVs reach their upper limits. This implies that the profit is pretty low if T_C is very small. The extreme scenario is that $T_C = 0$, which is identical with that without controllable load, and shows positive yearly profit only before 14th year.

Microgrid reliability with different T_C is shown in Table 6. The results are based on the scenario in the 10th year with $P_W = P_S = 150\,\text{kW}, P_B = 220\,\text{kWh}$ and the percent of controllable load is 20%.

From the results in Table 6, it can be seen that the reliability of the studied microgrid will decrease when small T_C is adopted for the DLC. Especially, the reliability is lower than $R_{\min}$ when T_C is smaller than 12 h. Test results presented above demonstrate the capability of the proposed expansion planning framework for studying important influence of controllable load. By carefully adjusting the control scheme of time shifting loads, we can enhance the efficiency and reliability of the isolated microgrid at the same time and prolong its expansion effectively.

6 Conclusion

In this paper, a tri-level expansion planning framework considering controllable loads is proposed for isolated microgrids, which is composed of demand expansion, capacity optimisation, and operation optimisation. The demand expansion is used to obtain the maximum load demand that the microgrid can supply. In capacity optimisation, optimal capacity configurations of DGs and controllable loads are determined for each planning year. Moreover, controllable loads are carefully modelled and considered in the proposed expansion planning. Case studies based on Weizhou Island in Guangxi Province validate the proposed models and methods. Especially, it can be seen that controllable loads can increase the maximum load demand of the isolated microgrid as well as its yearly profit. The yearly profit is increased by around 25% by utilising controllable loads when renewable energy sources are not sufficient. Thus, this work demonstrates the importance of controllable loads and corresponding method for integrating their models into the long-term planning of microgrids. Generally, when the negative annual profit is observed, the MG expansion should be stopped. However, if the load still wants to be integrated in this situation, the energy cost like electricity price should be raised to increase the microgrid profit.

The framework provides a general solution for optimal design of isolated microgrids and independent power systems in remote areas, in order to support long-term and sustainable developments of local economics by renewable energies. It can also be used for expansion planning of multi-energy systems, such as a CCHP. The tri-level design and the interactions among the three layers remain the same when the proposed method is applied to other kinds of systems. However, the operation optimisation formulation should be adjusted according to the features of the targeted system.

7 Acknowledgments

This work was supported by the NSFC under Grants 51477081 and 51621065, and the Tsinghua University Initiative Scientific Research Program under Grant 2012Z02140.

8 References

[1] Zhao, B., Zhang, X., Li, P., *et al.*: 'Optimal sizing, operating strategy and operational experience of a stand-alone microgrid on Dongfushan Island', *Appl. Energy*, 2014, **113**, pp. 1656–1666

[2] Zhou, W., Lou, C., Li, Z., *et al.*: 'Current status of research on optimum sizing of stand-alone hybrid solar-wind power generation systems', *Appl. Energy*, 2010, **87**, pp. 380–389

[3] Chen, L., Mei, S.: 'An integrated control and protection system for photovoltaic microgrids', *CSEE J. Power Energy Syst.*, 2015, **1**, pp. 36–42

[4] Li, G., Wenjian, L., Bingqi, J., *et al.*: 'Multi-objective stochastic optimal planning method for stand-alone microgrid system', *IET Gener. Transm. Distrib.*, 2014, **8**, pp. 1263–1273

[5] Prodromidis, G.N., Coutelieris, F.A.: 'A comparative feasibility study of stand-alone and grid connected RES-based systems in several Greek Islands', *Renew. Energy*, 2011, **36**, pp. 1957–1963

[6] Hou, P., Hu, W., Chen, Z.: 'Optimisation for offshore wind farm cable connection layout using adaptive particle swarm optimisation minimum spanning tree method', *IET Renew. Power Gener.*, 2016, **10**, pp. 694–702
[7] Chen, C., Wang, J., Kishore, S.: 'A distributed direct load control approach for large-scale residential demand response', *IEEE Trans. Power Syst.*, 2014, **29**, pp. 2219–2228
[8] Guo, L., Liu, W., Cai, J., *et al.*: 'A two-stage optimal planning and design method for combined cooling, heat and power microgrid system', *Energy Convers. Manage.*, 2013, **74**, pp. 433–445
[9] Khodaei, A., Bahramirad, S., Shahidehpour, M.: 'Microgrid planning under uncertainty', *IEEE Trans. Power Syst.*, 2014, **30**, pp. 2417–2425
[10] Wang, Z., Chen, Y., Ke, S., *et al.*: 'Optimal design of isolated microgrid considering run-time load controllability'. 2013 IEEE Region 10 Conf., Xi'an, 2013, pp. 1–6
[11] Soroudi, A., Amraee, T.: 'Decision making under uncertainty in energy systems: State of the art', *Renew. Sustain. Energy Rev.*, 2013, **28**, pp. 376–384
[12] Wang, Z., Chen, B., Wang, J., *et al.*: 'Robust optimization based optimal DG placement in microgrids', *IEEE Trans. Smart Grid*, 2014, **5**, pp. 2173–2182
[13] Hajipour, E., Bozorg, M., Fotuhi-Firuzabad, M.: 'Stochastic capacity expansion planning of remote microgrids with wind farms and energy storage', *IEEE Trans. Sustain. Energy*, 2015, **6**, pp. 491–498
[14] Nikmehr, N., Najafi Ravadanegh, S.: 'Heuristic probabilistic power flow algorithm for microgrids operation and planning', *IET Gener. Transm. Distrib.*, 2015, **9**, pp. 985–995
[15] Haesen, E., Driesen, J., Belmans, R.: 'Robust planning methodology for integration of stochastic generators in distribution grids', *IET Renew. Power Gener.*, 2007, **1**, pp. 25–32
[16] Stein, M.: 'Large sample properties of simulations using Latin hypercube sampling', *Technometrics*, 1987, **2**, pp. 143–151
[17] Janssen, H.: 'Monte-Carlo based uncertainty analysis: Sampling efficiency and sampling convergence', *Reliability Eng. Syst. Safety*, 2013, **109**, pp. 123–132
[18] Yu, H., Chung, C.Y., Wong, K.P., *et al.*: 'Probabilistic load flow evaluation with hybrid Latin hypercube sampling and Cholesky decomposition', *IEEE Trans. Power Syst.*, 2009, **2**, pp. 661–667
[19] Hakimi, S.M., Moghaddas-Tafreshi, S.M.: 'Optimization of smart microgrid considering domestic flexible loads', *J. Renew. Sustain. Energy*, 2012, **4**, p. 042702
[20] Chen, C., Wang, J., Heo, Y., *et al.*: 'MPC-based appliance scheduling for residential building energy management controller', *IEEE Trans. Smart Grid*, 2013, **4**, pp. 1401–1410
[21] Vlot, M.C., Knigge, J.D., Slootweg, J.G.: 'Economical regulation power through load shifting with smart energy appliances', *IEEE Trans. Smart Grid*, 2013, **4**, pp. 1705–1712
[22] Sanseverino, E.R., Di Silvestre, M.L., Zizzo, G., *et al.*: 'Energy efficient operation in smart grids: optimal management of shiftable loads and storage systems'. 2012 SPEEDAM, 2012, pp. 978–982
[23] Tasdighi, M., Ghasemi, H., Rahimi-Kian, A.: 'Residential microgrid scheduling based on smart meters data and temperature dependent thermal load modeling', *IEEE Trans. Smart Grid*, 2014, **5**, pp. 349–357
[24] Hakimi, S.M., Moghaddas-Tafreshi, S.M.: 'Optimal planning of a smart microgrid including demand response and intermittent renewable energy resources', *IEEE Trans. Smart Grid*, 2014, **5**, pp. 2889–2900
[25] Zhong, H., Xie, L., Xia, Q.: 'Coupon incentive-based demand response: Theory and case study', *IEEE Trans. Power Syst.*, 2013, **2**, pp. 1266–1276
[26] Shengwei, M., Yingying, W., Feng, L., *et al.*: 'Game approaches for hybrid power system planning', *IEEE Trans. Sustain. Energy*, 2012, **3**, pp. 506–517
[27] Koh, L.H., Wang, P., Choo, F.H., *et al.*: 'Operational adequacy studies of a PV-based and energy storage stand-alone microgrid', *IEEE Trans. Power Syst.*, 2015, **30**, pp. 892–900
[28] Doherty, R., O'Malley, M.: 'A new approach to quantify reserve demand in systems with significant installed wind capacity', *IEEE Trans. Power Syst.*, 2005, **2**, pp. 587–595
[29] Gavanidou, E.S., Bakirtzis, A.G.: 'Design of a stand-alone system with renewable energy sources using trade off methods', *IEEE Trans. Energy Convers.*, 1992, **7**, pp. 42–48
[30] Eberchart, R.C., Kennedy, J.: 'Particle swarm optimization'. Proc. of IEEE Int. Conf. on Neutral Networks, 1995, pp. 1942–1948